

Light Spring amplification in a multi-frequency Raman amplifier

J. A. Arteaga¹, A. Serbeto¹, K. H. Tsui¹, J. T. Mendonça²

¹*Instituto de Física, Universidade Federal Fluminense,*

Campus da Praia Vermelha, Niterói, RJ, 24210-346, Brasil, and*

²*IPFN, Instituto Superior Técnico, Universidade de Lisboa, 1049-001 Lisboa, Portugal*

Abstract

We propose to amplify and compress an ultrashort Light Spring laser seed with a long Gaussian-shaped laser pump through Raman amplification. This Light Spring, which has a helical spatio-temporal intensity profile, can be built on the superposition of three distinct laser frequency components. In order to get an independent frequency amplification, two criteria are established. Besides these criteria, a non equal frequency separation is necessary to avoid resonance overlapping when three or more frequencies are involved. The independent set of equations, which describes the wave-wave interaction in a plasma, is solved numerically for two different Light Spring configurations. In both cases, the amplification and transversal compression of the seed laser pulse have been observed, with a final profile similar to that of the usual Gaussian-shaped seed pulses. In addition, two different kinds of helical plasma waves are excited.

* johnny@if.uff.br

I. INTRODUCTION

Since the idea proposed by Malkin et al. [1] to improve the actual laser intensity by compression mechanism of the scattered laser beam in plasma through the stimulated Raman backscattering, many techniques have been explored to mitigate many unwanted effects. Such techniques include chirping the laser seed frequency [2], imposing laser coherence conditions after the amplification [3], and controlling of the laser parameters to extend the Backward Raman Amplification beyond the transversal relativistic instability [4], where a Gaussian-shape laser seed is amplified and compressed in a final horseshoe-shape [5]. On the other hand, Barth and Fisch [6] have introduced the concept of multi-frequency Raman amplifier to obtain a high efficiency Raman amplification using a laser seed wave packet with two separated frequencies, in a similar way to single-frequency seed pulse. In this case two criteria are established in order to avoid resonance overlap.

The advent of a new class of lasers with a donut-shaped intensity profile with a helical phase gives rise to many applications in different branches of laser science. These kinds of laser beam have been conceived by Allen et al. [7] in such a way that are well described by a family of Laguerre-Gaussian (LG) modes, which have the capability to carry and transfer the Orbital Angular Momentum (OAM) to matter [8]. Specifically, in a Raman amplifier, Viera et al. [9] using a Particle-in-cell (PIC) simulation describe various scenarios of OAM transfer to a Langmuir plasma wave using a LG pump and a seed laser, where the total OAM gained by the plasma wave corresponds to the difference of OAM among the pump and seed lasers, i.e., $\ell_w \hbar - \ell_s \hbar = \ell_p \hbar$ [10].

In order to get closer to the new generation of ultra high laser intensity, it is mandatory that the laser seed pulse, in a Raman amplifier, should have an ultrashort temporal duration, of the order of femtoseconds or attoseconds, leading to a broad frequency spectrum inside the wave packet. In this sense, Pariente and Qu  r   [11] have introduced the idea of linearly correlated frequencies inside the pulse with the modal index ℓ of the superposed LG modes, which gives a spatio-temporal correlated Light Spring (LS). This LS beam has the special feature that both intensity and phase get the same helical structure. These have recently been used to excite a twisted plasma wake-field in laser-plasma interaction studies [13], capable of accelerating helical electron beams.

In this paper, the concept of using an ultrashort LS laser as a seed interacting with a Gaussian pump laser in a cold plasma through the Raman backscattering mechanism is introduced. This will lead to the amplification and compression of the LS signal.

II. MULTI-FREQUENCY RAMAN AMPLIFIER

Basically, a single frequency Raman backward amplifier in a cold and under-dense plasma can be expressed in the paraxial approximation by the following set of three-wave coupled equations:

$$\left(-\frac{ic^2}{2\omega_1}\nabla_{\perp}^2 + \frac{\partial}{\partial t} + c\frac{\partial}{\partial z}\right)a_1 = \sqrt{\frac{\omega_1\omega_p}{2}}\hat{f}_1 b_1 \quad (1)$$

$$\left(-\frac{ic^2}{2\omega_1}\nabla_{\perp}^2 + \frac{\partial}{\partial t} - c\frac{\partial}{\partial z}\right)b_1 = -\sqrt{\frac{\omega_1\omega_p}{2}}\hat{f}_1^* a_1 \quad (2)$$

$$\left(-\frac{iS_e^2}{2\omega_p}\nabla_{\perp}^2 + \frac{\partial}{\partial t} - \frac{k_{f_1}}{\omega_{f_1}}S_e^2\frac{\partial}{\partial z}\right)\hat{f}_1 = -\sqrt{\frac{\omega_1\omega_p}{2}}a_1 b_1^*, \quad (3)$$

where a_1, b_1 are the normalized vector potentials for a circular polarized electromagnetic pump wave propagating along z-axis and a counter-propagating electromagnetic seed, respectively; while $\hat{f}_1 = -ick_{f_1}(\omega_1/2\omega_p^2)^{1/2}\delta n_1/n_0$ is the normalized electrostatic field of the Langmuir plasma wave, where k_{f_1} is the longitudinal plasma wavenumber, $\omega_p = (4\pi n_0 e^2/m)^{1/2}$ is the plasma frequency, n_0 is the equilibrium plasma density, δn_1 is the perturbed plasma density and $S_e = \sqrt{3T_e/m_e}$ is the electron thermal velocity. Here, the Raman backscattering matching conditions are $\omega_{a_1} = \omega_{b_1} + \omega_{f_1}$ and $k_{a_1} = k_{b_1} + k_{f_1}$, whose the dispersion relations are $\omega_{a_1, b_1} = \sqrt{c^2 k_{a_1, b_1}^2 + \omega_p^2}$ and $\omega_{f_1} = \sqrt{\omega_p^2 + S_e^2 k_{f_1}^2}$. In Eqs (1)-(3) the under-dense cold plasma approximation have been used leading to $\omega_1 \equiv \omega_{a_1} \approx \omega_{b_1} \approx ck_{b_1}$, $\omega_{f_1} \approx \omega_p$, and $k_{f_1} = k_{a_1} + k_{b_1} \approx 2\omega_1/c$.

According to Ref. [6], in a multi-frequency Raman amplifier, two conditions are imposed in order to avoid overlap and get an independent amplification. The first one is that the nearest separation frequency has to be greater than the maximum bandwidth gain acquired by each mode, in the linear Raman stage (not pump depletion), that is, $\Delta = \omega_j - \omega_i > \max\{a_j \sqrt{\omega_j \omega_p / 2}\}$ [14]. The second condition is that the pulse duration, τ_{FWHM} , should be greater than the period of the resulting beat wave, that is, $\tau_{FWHM} > 2\pi/\Omega_{ji} = 4\pi/(\omega_j - \omega_i)$. Here, we will consider three frequency components to describe the pump and seed wave packet, such that the frequency separation is given by

$$\omega_2 - \omega_1 = \Delta, \quad \omega_3 - \omega_2 = \omega_2 - \omega_1 + \delta, \quad (4)$$

where the meaning of δ is explained a posteriori.

The total normalized potential vectors of the pump and seed are described by

$$\vec{a} = \frac{1}{\sqrt{2}} \text{Re} \left(\sum_{j=1}^3 a_j e^{i(\omega_j t - k_j z)} \hat{e} \right), \quad \vec{b} = \frac{1}{\sqrt{2}} \text{Re} \left(\sum_{j=1}^3 b_j e^{i(\omega_j t + k_j z)} \hat{e} \right) \quad (5)$$

where $\hat{e} = (\hat{x} + i\hat{y})/2$ is the circular polarization vector. The matching conditions are given by

$$\omega_{a_j} = \omega_{b_j} + \omega_{f_j}, \quad k_{f_j} = k_{a_j} + k_{b_j}, \quad \text{for } j = 1, 2, 3, \quad (6)$$

with $\omega_{a_j, b_j} = \sqrt{c^2 k_{a_j, b_j}^2 + \omega_p^2}$ and $\omega_{f_j} = \sqrt{\omega_p^2 + S_e^2 k_{f_j}^2}$. The under-dense cold plasma approximation leads to $\omega_{a_j, b_j} \approx ck_{a_j, b_j}$, making the down-shifted frequency negligible, i.e, $\omega_{b_j} \approx \omega_{a_j} \equiv \omega_j$. Hence, the set of equations to describe three independent Raman amplifiers is given by

$$\hat{D}_{P_j} a_j = \sqrt{\frac{\omega_j}{\omega_1}} \hat{f}_j b_j, \quad (7)$$

$$\hat{D}_{S_j} b_j = \sqrt{\frac{\omega_j}{\omega_1}} \hat{f}_j^* a_j, \quad (8)$$

$$\hat{D}_{L_j} \hat{f}_j = -\frac{\omega_p}{\omega_{f_j}} \sqrt{\frac{\omega_j}{\omega_1}} a_j b_j^*, \quad \text{for } j = 1, 2, 3, \quad (9)$$

where $\hat{D}_{P,S,L}$ are the differential operators associated to the pump, seed and Langmuir waves defined as follows

$$\hat{D}_{P,S_j} = -\frac{i}{\sqrt{8}} \frac{\sqrt{\omega_1 \omega_p}}{\omega_j} \bar{\nabla}_\perp^2 + \frac{\partial}{\partial t'} + \hat{k}_{p,s} \frac{\partial}{\partial z'}, \quad (10)$$

$$\hat{D}_{L_j} = -\frac{i}{\sqrt{8}} \frac{S_e^2}{c^2} \frac{\sqrt{\omega_1 \omega_p}}{\omega_{f_j}} \bar{\nabla}_\perp^2 + \frac{\partial}{\partial t'} - \frac{k_{f_j}}{\omega_{f_j}} \frac{S_e^2}{c} \frac{\partial}{\partial z'}, \quad (11)$$

with $\hat{k}_p = +1$ and $\hat{k}_s = -1$. Here, the time and space variables are normalized with $\sqrt{\omega_1 \omega_p}/2$ and $\sqrt{\omega_1 \omega_p}/2/c$, respectively. We should point out that in Eqs (7-9) the coupling between the envelopes is only for the same j -mode. In this set of equations the non-resonant terms, which correspond to coupling with different j -modes, are neglected since other Raman decay processes are avoided, that is, $\omega_j \neq \omega_i + \omega_p$ for $i \neq j$, leading to $\omega_p \neq \{\Delta, \Delta + \delta, 2\Delta + \delta\}$. As we can see, on the right-hand-side (RHS) of Eqs (7 - 9) we have complex exponential terms whose arguments are given by $k_{a_i} + k_{b_j} - k_{f_k} \approx k_i + k_j - 2k_k$, for $i \neq j \neq k$. Then, in order to avoid cross resonance, these arguments can not be null. This condition gives us the necessary requirement of non equal separation among the frequencies ω_1 and ω_3 , respect to the central frequency, ω_2 , which corresponds

to taking a small frequency shifting, δ , as given by Eq. (4). For $\delta \neq 0$, it gives us fast phase terms, such as $\exp(i(k_3 + k_1 - 2k_2)z) \approx \exp(2i\delta z/c)$ and others, which on average, do not contribute to the Raman resonant amplification.

III. LIGHT SPRING

Following Ref. [11], a LS beam can be generated when each frequency inside the laser pulse is correlated with the LG modal index ℓ , according to

$$\ell(\omega) = \ell_0 + \frac{\Delta\ell}{\Delta\omega}(\omega - \omega_0), \quad (12)$$

where ω_0 is the central frequency corresponding to a modal index ℓ_0 , $\Delta\omega$ is the spectral width, and $\Delta\ell$ is the variation of the modal index through $\Delta\omega$. The correlation given by Eq. (12) results in a beat wave with a helical intensity profile, whose temporal pitch is given by $\tau_p = 2\pi\Delta\ell/\Delta\omega$. Considering two kinds of LS beam, which are uniquely differentiated by the slope, $\Delta\ell/\Delta\omega$, as detailed in Fig. 1, the superposition of the three modes is represented as

$$b = \sum_{j=1}^3 B_j(r, t) e^{\varphi_j(r, \theta, z)}, \quad (13)$$

where

$$B_j = B_{0j}(z, t) w_{0j} \sqrt{\frac{2p_j!}{\pi w_j^2 (p_j + |\ell_j|)!}} \left(\frac{\sqrt{2}r}{w_j} \right)^{|\ell_j|} L_p^{\ell_j} \left(\frac{2r^2}{w_j^2} \right) e^{-r^2/w_j^2}, \quad (14)$$

is the LG mode amplitude and

$$\varphi_j = i \left[\frac{R_j z r^2}{z_{0j}^2 + R_j^2} - (2p_j + |\ell_j| + 1) \arctan(z/z_{0j}) + \ell_j \phi \right], \quad (15)$$

is the respective screw phase. Here B_{0j} represents the amplitude of each mode and $w_{0j} = z_{0j}(1 + R_j^2 z^2 / z_{0j}^2)$ is the normalized transverse waist, which is a function of the normalized Rayleigh length, $z_{0j} = w_{0j}^2$. In this equation, for $\ell = 0$, we have the Gouy phase, which gives the curvature evolution of the wavefront, with $R_j = \sqrt{\omega_1 \omega_p} / \omega_j$. The last term in φ_j generates the helical structure of the LG mode, with ℓ being the modal index, which gives us the amount of OAM carried by the mode.

This set of coupled equations (7-9) is independently solved for each j -mode, for the two cases

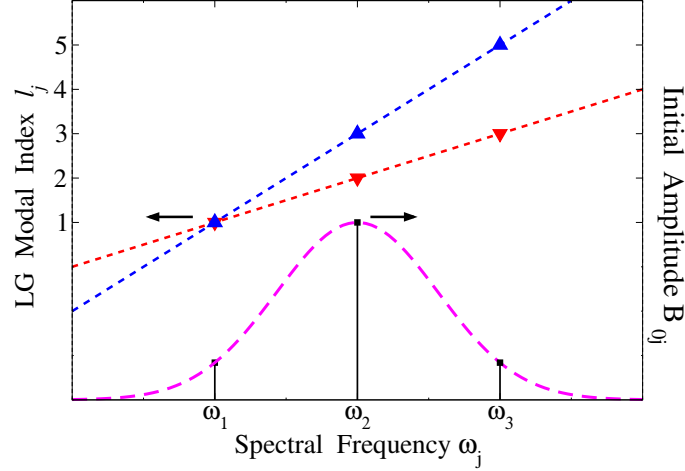


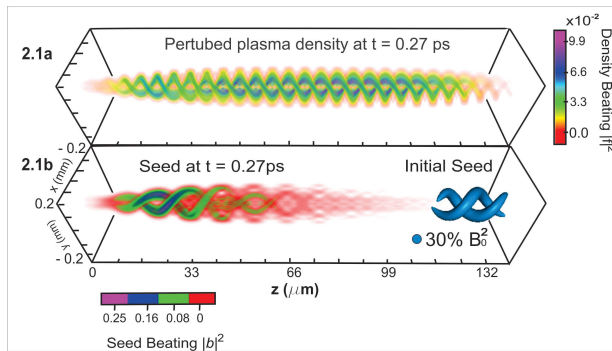
Figure 1: Two modal correlation indexes with different slopes for a seed pulse composed by three frequencies (pink dotted line). The first one has a slope $\Delta\ell/\Delta\omega = 2$ (blue dotted line) with integer modal indexes $\{1, 3, 5\}$. The second case, $\Delta\ell/\Delta\omega = 1$ (red dotted line) with integer modal indexes $\{1, 2, 3\}$. In both cases, each mode has an initial Gaussian profile, where the modes with frequencies ω_1 and ω_3 , respectively, have an amplitude corresponding to 20% of the central mode ω_2 .

mentioned in Fig. (1). Hence, the final beat wave amplitude will be given by the superposition of each envelope amplitude, i.e, for the beat wave seed we have $\vec{b} = \sum_j \vec{b}_j$. For simplicity we will consider an initial transverse waist $w_j = w_{0,j} = w_0$ large enough to avoid diffraction effects on the seed laser pulse during the interaction time. Also, the LG modes will be considered to have only one ring in its intensity profile, in such a way that $p_j = 0$. The pump laser pulse will be assumed to have a Gaussian transversal structure with the same waist of the seed pulse and have a temporal duration of picoseconds, in order to have the Raman process reaching the nonlinear stage. Here we will consider a plasma with an electron temperature $T_e = 5\text{eV}$, electron density $n = 5 \times 10^{18} \text{ cm}^{-3}$ ($\omega_p \approx 126 \text{ THz}$), central frequency $\omega_2 = 2\pi \times 375 \text{ THz}$ ($\lambda \sim 0.8\mu\text{m}$), low frequency $\omega_1 = 2\pi \times 345 \text{ THz}$ and high frequency $\omega_3 = (2\pi \times 405 + 1) \text{ THz}$. With these frequencies, we have the frequency shift, $\Delta = 2\pi \times 30 \text{ THz}$, and a small mismatching parameter, $\delta = 1 \text{ THz}$. The initial central seed mode is assumed to have an amplitude $B_{02} = 2 \times 10^{-2}$, while the initial pump amplitude is set at $a_j = a_0 = 0.1$, leading to $\max\{4a_j \sqrt{\omega_j \omega_p / 2}\} = 4a_0 \sqrt{\omega_3 \omega_p / 2} \approx 1.6 \times 10^{14} < \Delta$, which satisfies the first criteria for a multi-frequency Raman interaction. For the second criteria, each mode that composes the pulse has a temporal duration $\tau_{FWHM} = 84fs > 2\pi\Omega_{ij} = 33fs$, which is also satisfied. On the right side of Figures 2.1b and 2.2b, the initial LS seeds are presented for the two cases of slope respectively mentioned in Figure 1. Each slope produces one kind of LS as is reported in [11], where for the case $\Delta\ell/\Delta\omega = 1$ (Fig. 2.2b) the seed LS presents only one coil,

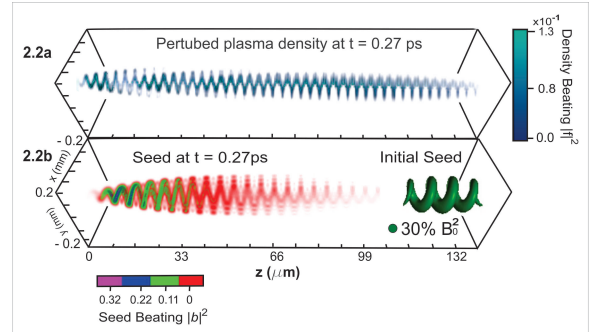
while for $\Delta\ell/\Delta\omega = 2$ (Fig 2.1b) two intertwined coils are generated. These LS structures on the intensity profile are described by the beating of the three near frequency modes as follows

$$\vec{b} \cdot \vec{b}^* = |\vec{b}|^2 = \sum_{j=1}^3 |b_j|^2 + 2\text{Re} \left\{ \sum_{\substack{i,j \\ i \neq j, i > j}}^3 b_i b_j^* e^{i[(k_j - k_i)z - (\omega_j - \omega_i)t]} \right\} \quad (16)$$

In both cases, during the non linear stage, the LS seed is amplified and compressed in the front of the pulse as is represented in Figs. 2.1b and 2.2b. Fig. 3.1 shows the iso-surface (orange), at left of the box, taken at 25% from the final maximum value of the seed, and at right of the box, the iso-surface (blue) taken at 25% of the seed initial maximum value. Similarly, Fig. 3.2 represents the final (purple) and initial (green) iso-surfaces for one coil seed. Inside the gray surface in Figs 3.1 and 3.2 is the leading pulse of the seed that looks very similar to the horseshoe shape of the conventional Gaussian-shape pulses [5, 9] because of the transverse compression in its front. Outside the gray surface we can observe the formation of a second spring that keeps the same feature of the leading spring but with less intensity corresponding to the sub-pulses generated by the energy exchange during Raman interaction. Figs. 2.1a and 2.2a show the beat wave generated by the three perturbed modes of the plasma density, which are computed in the same way as in Eq.(16). In both cases, the perturbed plasma density acquires a helical structure according to the kind of the LS seed, obeying the individual OAM conservation [10], and keeping the same properties of the conventional one frequency Raman amplifier, that is, the density maximum is located in the same region of maximum seed beating.

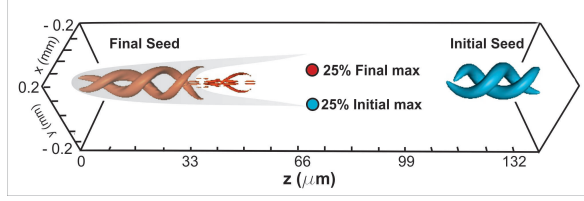


2.1. Slope $\Delta\ell/\Delta\omega = 2$

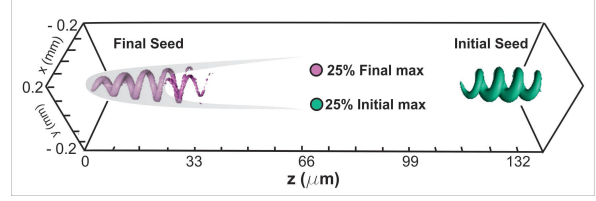


2.2. Slope $\Delta\ell/\Delta\omega = 1$

Figure 2: Figures 2.1a and 2.2a show the final intensity profile of the perturbed plasma wave. Figures 2.1b and 2.2b, at right side, show the isosurface corresponding to 30% of the initial peak laser seed intensity, which final intensity profile is presented at left side.



3.1. Slope $\Delta\ell/\Delta\omega = 2$



3.2. Slope $\Delta\ell/\Delta\omega = 1$

Figure 3: Seed iso-surfaces for the initial and final stages for the cases in Fig 2.1b and Fig 2.2b. For both cases we have a iso-surface taken at the 25% of the initial and final maximum value. The horse-shoe shape of the main pulse is represented by the gray surface in the final stage of both cases.

IV. CONCLUSIONS

In conclusion, we have implemented a LS seed pulse through the correlation of the spectral width with the modal index from the LG modes. It is verified that, depending on the slope $\Delta\ell/\Delta\omega$, various intertwined coils can be generated by the spring. It is important to note that, as represented by the blue and red dotted lines in Fig 1, along the spectral frequency of the pulse there exists a continuum of frequencies that is correlated according to Eq.(12), which leads to a large number of non integer modal index that are not solutions of the paraxial equation. These non integer modes cause the diffraction on the edge of LS, while keeping its helical structure, as discussed in Refs. [11, 12, 15]. With respect to the dynamics of the LS seeds, we employ a triple Raman amplifier where the separation between each mode has to satisfy some minimum requirements to get its independence. These requirements were proposed and tested by analyzing the Fourier spectrum in a 1D PIC simulation for a single, double and triple Raman amplifier [6]. Also, in a multi-frequency Raman scheme, when the down shifted frequency is neglected, i.e $\omega_{a_j} = \omega_{b_j}$, the separation between a neighboring pair of frequencies has to be different from another pair as given by the δ factor defined in Eq.(4), which supports the individual evolution of our triple wave interaction model. From the well known shape of a single-frequency Raman amplifier, the transversal compression of the initial LS laser seed gives rise to what we call a *horseshoe Light Spring*. However, when we compare the thickness of the final and initial iso-surfaces in Figs. 3.1 and 3.2, these are essentially the same, opposing to the already known longitudinal compression in the non linear stage of a single-frequency Raman [1]. It may be presumably related to the broadening suffered by each mode in the linear Raman stage, given by $a_j \sqrt{\omega_j \omega_p}$, that depends on the mode frequency ω_j , leading to different compression rates and causing the maximum of the lower frequencies slipping ahead of the highest one. Also, the transverse coupling between the Gaussian-shape pump

with each of the seed mode is different because of the vortex size is proportional to the amount of OAM carried by each mode. In addition, we have shown the possibility of having a spiral phase in a plasma wave and a helical profile in its intensity. This opens the possibility of applying this technique to generate helical electron beams [16, 17]. Finally, we are conscious of the limitations in the three wave interaction scheme discussed here. In order to predict with more accuracy the dynamics of the process, it is mandatory to use 3D PIC simulations to check if the longitudinal compression occurs, and to explore the effect of instabilities on the LS beam in a multi frequency Raman scheme.

ACKNOWLEDGMENT

We thank Kenan Qu, Qing Jia and Nathaniel Fisch, from University of Princeton, for their fruitful comments to develop this work, and Martin Silva for graphic support. This research is supported by the National Council of Research and Technological Development (CNPQ) of Brazil

-
- [1] V. M. Malkin, G. Shvets, and N. J. Fisch *Phys. Rev. Lett.*, 82, 4448 (1999)
 - [2] Z. Toroker, V. Malkin, and N. J. Fisch, *Phys. Rev. Lett.*, 109, 085003 (2012)
 - [3] M. R. Edwards, K. Qu, J. M. Mikhailova, and N. J. Fisch, *Physics of Plasmas*, 24, 103110 (2017)
 - [4] V. M. Malkin, Z. Toroker, and N. J. Fisch *Phys. Rev. E*, 90, 063110 (2014)
 - [5] R. M. G. M. Trines, F. Fiúza, R. Bingham, R. A. Fonseca, L. O. Silva, R. A. Cairns and P. A. Norreys *Nature Physics*, 7, 87 (2011)
 - [6] I. Barth and N. J. Fisch, *Phys. Rev. E*, 97, 033201 (2018)
 - [7] L. Allen, M. W. Beijersbergen, R.J.C Spreeuw, J. P. Woerdman *Phys. Rev. A*, **45**, 8185 (1992).
 - [8] A. Yao and M. Padgett, *Adv. Opt. Photon.*, **3**, 161 (2011)
 - [9] J. Vieira, R. M. G. M. Trines, E. P. Alves, R. A. Fonseca, J. T. Mendonça, R. Bingham, P. Norreys, L. O. Silva *Nature Communications*, **7**, 10371 (2016)
 - [10] J. T. Mendonça, B. Thidé, H. Then , *Phys. Rev. Letters*, **102**, 185005 (2009)
 - [11] G. Pariente and F. Quéré *Optics Letters* , 40, 9 (2015)
 - [12] J. T. Mendonça, A. Serbeto and J. Vieira, *Sc. Rep.*, 8, 7817 (2018).
 - [13] J. Vieira, J. T. Mendonça, and F. Quéré, *Phys. Rev. Lett.*, 121, 054801 (2018)

- [14] V. M. Malkin, G. Shvets, and N. J. Fisch, *Physics of Plasmas*, 7, 2232, (2000)
- [15] M. V. Berry *J. Opt. A: Pure Appl. Opt.*, 6, 259 (2004)
- [16] E. Hemsing, A. Knyazik, M. Dunning, D. Xiang, A. Marinelli, C. Hast, J. B. Rosenzweig *Nature Physics*, **9**, 549 (2013).
- [17] J. A. Arteaga, A. Serbeto, J. T. Mendonça, K. H. Tsui, and L. F. Monteiro *Physics of Plasmas*, 24, 123108 (2017)